

# Evaluation of Anechoic Chamber for EMI over 1GHz by Pseudo Plane-Wave Spectrum

<sup>#</sup>Michitaka Ameya <sup>1</sup>, Satoru Kurokawa <sup>1</sup>

Ikuo Watanabe <sup>2</sup>, Mikito Yamaguchi <sup>2</sup>, Ryoichi Hasumi <sup>2</sup>

<sup>1</sup>National Institute of Advanced Industrial Science and Technology,  
1-1-1 Umezono, Tsukuba, Ibaraki, 305-8563 Japan, m.ameya@aist.go.jp

<sup>2</sup>DEVICE Co. Ltd.,  
1170-1 Hirota, Kohnosu, Saitama, 365-0005 Japan, sales@deviceco.co.jp

## 1. Introduction

Recently, site evaluation of anechoic chamber for EMI over 1GHz has attracted much attention because EU and VCCI start the regulation for EMI above 1GHz from October 2010. Although there are a lot of evaluation methods for anechoic chamber [1] [2], CISPR16-1-4[3] defines an evaluation method, SVSWR method, for EMI anechoic chamber over 1GHz. The SVSWR is measured at the only four positions (front, right, left, and center) at the height above a turntable of 1 m. Only these positions may not be enough for the reflection analysis of anechoic chambers for EMI over 1GHz. In this paper, we propose a new site evaluation method using pseudo plane-wave spectrum. The proposed method enables to obtain the intensity and the angle of arrival of reflection waves and facilitates improving performance of anechoic chambers.

## 2. Plane-Wave Spectrum and Pseudo Plane-Wave Spectrum

According to the electromagnetic wave theory [4], arbitrary electric field  $\mathbf{E}(x, y, z)$  can be expressed by superposition of plane-waves of the form  $\mathbf{X}(k_x, k_y)e^{-j(k_x x + k_y y + k_z z)}$ , which have the same frequency, different amplitudes, and are travelling in different directions. Thus the field  $\mathbf{E}(x, y, z)$  can be written as

$$\mathbf{E}(x, y, z) = \int_{-\infty}^{+\infty} \int_{-\infty}^{+\infty} \mathbf{X}(k_x, k_y) e^{-j(k_x x + k_y y + k_z z)} dk_x dk_y \quad (1)$$

while  $\mathbf{X}(k_x, k_y)$  is the vector plane-wave spectrum (PWS),  $x, y, z$  is the Cartesian coordinates of the electric field, and  $k_x, k_y, k_z$  is the wave number for each axis. These wave numbers are related to the direction of the plane-waves, the relationship between wave numbers and direction angle is

$$k_x = k \sin \theta \cos \phi, \quad k_y = k \sin \theta \sin \phi, \quad k_z = k \cos \theta \quad (2)$$

where  $k$  is the magnitude of wave vector  $\mathbf{k}$ ,  $k = |\mathbf{k}| = 2\pi / \lambda$ , and  $\theta, \phi$  indicate travelling directions of a plane-wave. By calculating two-dimensional Fourier transformation to the  $x$  and  $y$ , the PWS can be written as

$$\mathbf{X}(k_x, k_y) e^{-jk_z z} = \int_{-\infty}^{+\infty} \int_{-\infty}^{+\infty} \mathbf{E}(x, y, z) e^{+j(k_x x + k_y y)} dx dy \quad (3)$$

The field  $\mathbf{E}_{\text{reflect}}$  created by the reflected waves in the anechoic chamber is obtained from subtraction of the reference field  $\mathbf{E}_{\text{direct}}$ , which is an ideal no-reflection field (direct wave only), from the measuring target field  $\mathbf{E}_{\text{meas}}$  including direct wave and reflected waves. Therefore, the electric field consists of reflection waves at  $z = z_0$  and its PWS is expressed by

$$\mathbf{E}_{\text{reflect}}(x, y, z_0) = \mathbf{E}_{\text{meas}}(x, y, z_0) - \mathbf{E}_{\text{direct}}(x, y, z_0) \quad (4)$$

$$\mathbf{X}_{\text{reflect}}(k_x, k_y) e^{-jk_z z_0} = \int_{-\infty}^{+\infty} \int_{-\infty}^{+\infty} [\mathbf{E}_{\text{meas}}(x, y, z_0) - \mathbf{E}_{\text{direct}}(x, y, z_0)] e^{+j(k_x x + k_y y)} dx dy \quad (5)$$

The PWS of reflection waves,  $\mathbf{X}_{\text{reflect}}(k_x, k_y)$ , indicates the angular distribution of reflection waves. Therefore, we can estimate the intensity and the direction of arrival (DOA) of each reflection waves and facilitate improving performance of anechoic chambers.

Due to the difficulty of measuring electric fields directly, we use an antenna and the antenna factor for estimating the electric fields. The  $z$  component of the electric field,  $E_{z,\text{reflect}}(x, y, z_0)$ , and its PWS is expressed by

$$\begin{aligned} E_{z,\text{reflect}}(x, y, z_0) &= E_{z,\text{meas.}}(x, y, z_0) - E_{z,\text{direct}}(x, y, z_0) \\ &\approx AF[V_{\text{meas}}(x, y, z_0) - V_{\text{direct}}(x, y, z_0)] \end{aligned} \quad (6)$$

$$\frac{X_{z,\text{reflect}}(k_x, k_y)}{AF(\theta, \phi)} e^{-jk_z z_0} = \int_{-\infty}^{+\infty} \int_{-\infty}^{+\infty} [V_{\text{meas}}(x, y, z_0) - V_{\text{direct}}(x, y, z_0)] e^{+j(k_x x + k_y y)} dx dy \quad (7)$$

In practice, we cannot measure the electric field of infinite area ( $x, y = -\infty$  to  $+\infty$ ). Hence, two-dimensional Blackman window [5]  $w(x, y)$  is multiplied to the differential field  $E_{z,\text{reflect}}$ . Fourier transformation pair of two-dimensional Blackman window is shown in Figure 1. A vector network analyzer can measure the ratio of the input signal to the output signal easily, so the equation (7) is rewritten by  $S$ -parameter as

$$\begin{aligned} X'_{z,\text{reflect}}(k_x, k_y) e^{-jk_z z_0} &= e^{-jk_z z_0} \frac{X_{z,\text{reflect}}(k_x, k_y)}{V_{\text{in}} AF(\theta, \phi)} \otimes W(k_x, k_y) \\ &= \int_{y_{\min}}^{y_{\max}} \int_{x_{\min}}^{x_{\max}} w(x, y) [V_{\text{meas}}(x, y, z_0) - V_{\text{direct}}(x, y, z_0)] / V_{\text{in}} e^{+j(k_x x + k_y y)} dx dy \\ &= \int_{y_{\min}}^{y_{\max}} \int_{x_{\min}}^{x_{\max}} w(x, y) [S_{21,\text{meas}}(x, y, z_0) - S_{21,\text{direct}}(x, y, z_0)] e^{+j(k_x x + k_y y)} dx dy \end{aligned} \quad (9)$$

where  $X \otimes Y$  means the convolution of  $X$  and  $Y$ . We defined  $X'_{z,\text{reflect}}(k_x, k_y)$  as pseudo plane-wave spectrum (PPWS) for the reflection waves. Although PPWS is influenced by the antenna factor of the receiving antenna and the window function  $w(x, y)$ , the DOA information is still included in the PPWS. In a similar way, the PPWS of the measuring target field and the reference field is calculated by equation (10) and (11).

$$X'_{z,\text{meas}}(k_x, k_y) = e^{jk_z z_0} \int_{-y_{\min}}^{+y_{\max}} \int_{-x_{\min}}^{+x_{\max}} w(x, y) S_{21,\text{meas}}(x, y, z_0) e^{+j(k_x x + k_y y)} dx dy \quad (10)$$

$$X'_{z,\text{direct}}(k_x, k_y) = e^{jk_z z_0} \int_{-y_{\min}}^{+y_{\max}} \int_{-x_{\min}}^{+x_{\max}} w(x, y) S_{21,\text{direct}}(x, y, z_0) e^{+j(k_x x + k_y y)} dx dy \quad (11)$$

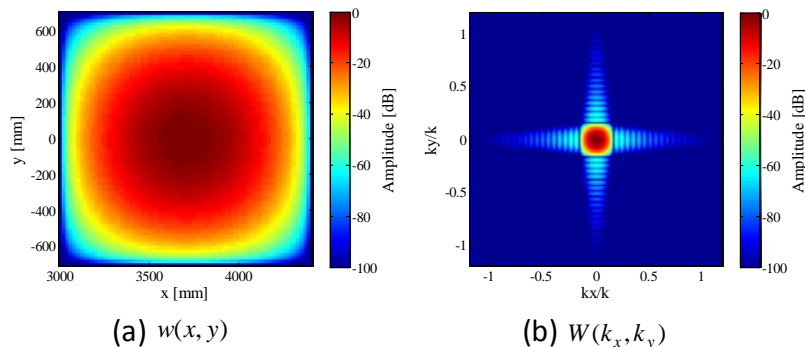


Figure 1: Fourier transformation pair of two-dimensional Blackman window

### 3. Measurement Setup for PPWS in Anechoic Chamber

Measurement setup is shown in Figure 2. We assume a turntable with 1.4 m diameter arranged on the center of 25 m length by 16 m width by 9 m height semi-anechoic chamber. The  $S_{21}$  distribution is measured along the measurement grid using XY field scanner shown in Figure 3(a). The grid interval is 20 mm for both  $x$  and  $y$  directions. The measurement area is from  $x = 3000$  mm

to 4400, and from  $y = -700$  mm to  $+700$  mm, the total measurement point is 5041 points (71 points by 71 points). For connecting the transmitting port and the receiving port of the VNA to the antenna, a 20 m coaxial cable and a 10 m coaxial cable are used. We use a double ridged waveguide horn antenna (ETS-Lindgren Model 3117) as a receiving antenna. The biconical broadband antenna (Schwarzbeck SBA9119) is employed as a transmitting antenna. The radiation pattern of the transmitting antenna is compliant with CISPR-16-1-4 specification according to the manufacture's datasheet [6].

To generate the reflection waves obviously, the reflecting object, which is a metal plate rested against a stepladder, is located near the absorber (red circle in the Figure 2). Figure 3(b) shows the measurement configuration with reflecting object. Only the vertical polarization is measured in this trial.

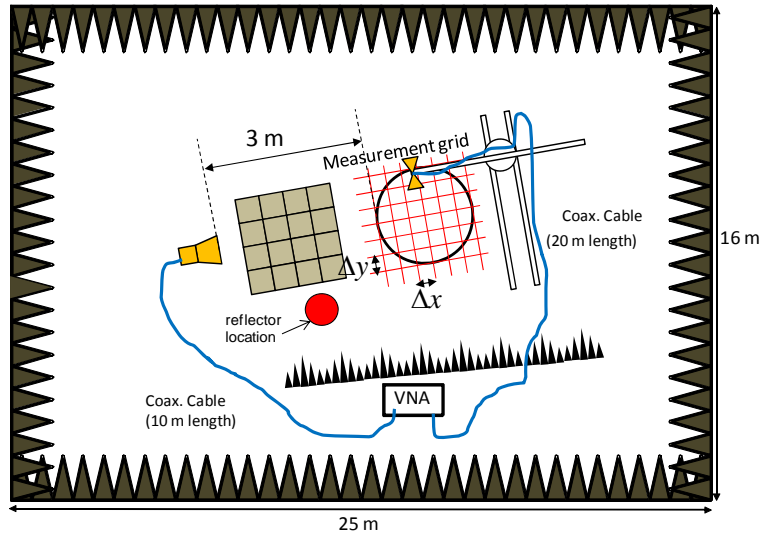
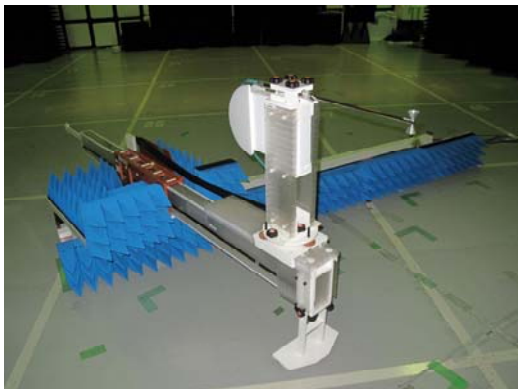
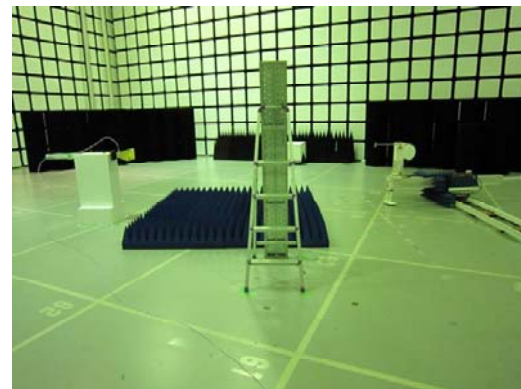


Figure 2: Measurement setup for PPWS



(a) XY field scanner



(b) Measurement setup with reflector

Figure 3: XY field scanner and measurement configuration with reflector

#### 4. Results

Figure 4 shows the distribution of measured target field, the reference field and the differential field between Figure 4(a) and 4(b). The measurement frequency is 4 GHz. From the figure 4(a), interference pattern is observed due to the reflecting wave from the reflector. The reference field is measured after removing the reflecting object, hence there is still interference pattern due to the small reflecting waves from the XY field scanner and the anechoic chamber walls.

Figure 5 shows the PPWS of the measured target field, the reference field and the differential field. From the Figure 5(c), the 1<sup>st</sup> maximum peak is observed at  $(k_x, k_y) = (-0.753, -0.656)$  and its intensity is  $-15.1$ dB compared to the direct wave intensity. The 2<sup>nd</sup>

maximum peak observed at  $(k_x, k_y) = (-1.0, 0.0)$  is a residual of the direct wave PPWS. The estimated DOA of the reflecting wave from the metal plate is  $\phi = 221^\circ$  from equation (2). This value almost agree with  $\phi = 219^\circ$  obtained by geometric calculation.

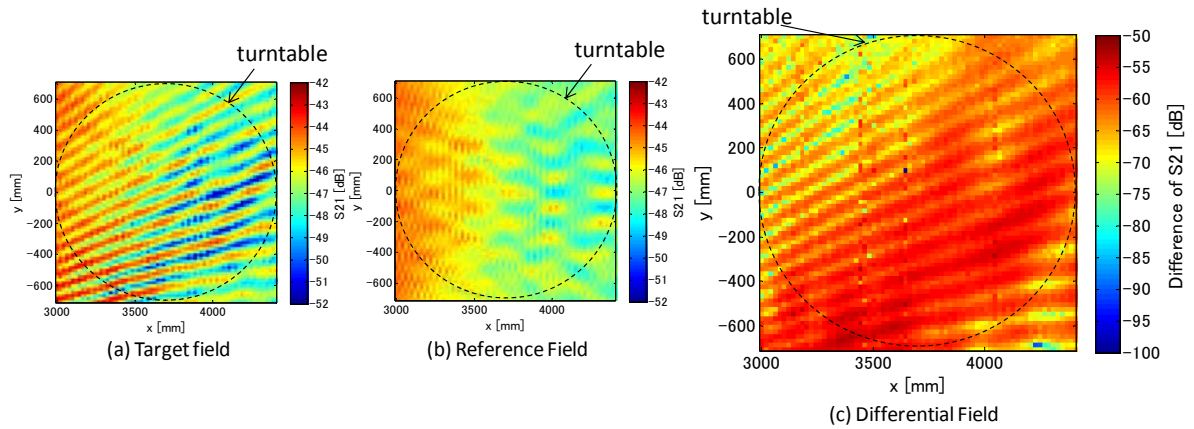


Figure 4: Measured  $S_{21}$  field, reference  $S_{21}$  field and the differential  $S_{21}$  field at 4 GHz

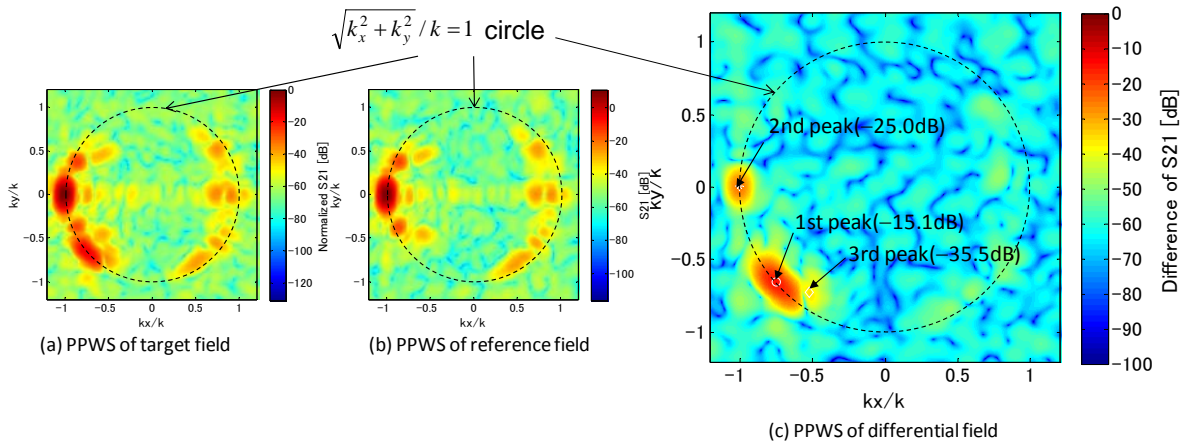


Figure 5: PPWS of measured  $S_{21}$  field, reference  $S_{21}$  field and the differential  $S_{21}$  field at 4 GHz

## 5. Conclusions

In this paper, we proposed a new evaluation approach for anechoic chamber using pseudo plane-wave spectrum. From the wave number of the peak in the PPWS distribution of differential field, the DOA of the reflecting wave can be estimated.

## References

- [1] J. Appel-Hansen, "Reflectivity Level of Radio Anechoic Chambers", IEEE Trans. on Ant. and Prop., vol.AP-21, no.4, July 1973.
- [2] B. B. Tian, "Free Space VSWR Method for Anechoic Chamber Electromagnetic Performance Evaluation", MI Technologies, Technical Papers, Nov.2008.
- [3] CISPR 16-1-4, "Specification for radio disturbance and immunity measuring apparatus and methods -Part 1-4: Radio disturbance and immunity measuring apparatus - Ancillary equipment -Radiated disturbances", Edition 2.1, 2008-01.
- [4] C. A. Balanis, Antenna Theory: Analysis and Design 3<sup>rd</sup> ed., John Wiley & Sons, New York, 2005.
- [5] Oppenheim, A.V., and R.W. Schafer, Discrete-Time Signal Processing, Upper Saddle River, NJ: Prentice-Hall, 1999, pp. 468-471.
- [6] Schwarzbeck Mess Elektronik, "Microwave Biconical Broadband Antenna SBA 9119", <http://www.schwarzbeck.de/Datenblatt/K9119.pdf>, accessed July 2010.